Complex-Induced Proximity Effects and Dipole-Stabilized Carbanions: Kinetic Evidence for the Role of Complexes in the α′-Lithiations of Carboxamides

David R. Hay, Zhiguo Song, Stanley G. Smith,* and Peter Beak*

Contribution from the Department of Chemistry, University of Illinois, Urbana, Illinois 61801.
Received November 19, 1987

Abstract: The kinetics of the α′-lithiations of *N,N*-dimethyl-2,4,6-triisopropylbenzamide (**4**) and *N,N*-diethyl-2,4,6-triisopropylbenzamide (**5**) by *sec*-butyllithium (*s*-BuLi) in cyclohexane have been investigated. Direct observation of the reactant amide, the intermediate amide–lithium reagent complex(es), and the α′-lithiated products by stopped-flow infrared spectroscopy was used to investigate the initial rate constants as a function of reactant concentrations. At constant amide concentration the initial rate constant decreases sharply with increasing concentration of *s*-BuLi. This behavior is also observed in the presence of tetramethylethylenediamine (TMEDA). The major interaction of TMEDA with *s*-BuLi in cyclohexane is shown by cryoscopic measurements to be an addition of TMEDA to aggregated *s*-BuLi. Semiquantitative schemes constructed on the basis of the kinetic data suggest the presence of at least two reactive complexes and that complexes with more ligands are more reactive. The implications of these results are discussed.

A reaction in which a carbon–hydrogen bond is broken with transfer of a proton from the substrate to an organolithium reagent is a key step in a wide variety of important sequences. Although formulation of the proton transfer as proceeding via a prereaction equilibrium association complex between the lithium of the reagent and a functional group of the substrate is consistent with schemes that have been proposed in organolithium chemistry for over 40 years, the evidence that such complexes are on the reaction pathway is usually inferential.[1] Thus, solid-state structures, spectroscopic studies of organolithium reagents in solution, reasonable explanations of regio- and stereoselectivities, and theory have been used to provide indirect support for the many proposals of such intermediates.[1-5] We have used this background recently to suggest a complex-induced proximity effect which unifies a number of novel and useful reactions in organolithium chemistry.[5]

Reaction kinetics has proven useful for delineation of reaction pathways of organolithium reagents, particularly for additions of organolithium compounds to carbonyl groups in which the intermediate complexes are directly observable.[6,7] The full and fractional kinetic orders that have been observed are consistent with reactions of aggregates and disassociated organolithium reagents in additions to carbonyl groups, to double bonds, and in halogen metal exchange.[6-9] In hydrocarbon solvents the most general pattern is reaction of aggregated species.[6,10] In the most carefully examined cases, pathways that involve different aggregates and/or dissociated reagents appear to be competitive.[6,7]

In this report, we detail our kinetic investigation of the proposal that the α′-lithiation of dialkylamides **1** with tetrameric *sec*-butyllithium (*s*-BuLi)$_4$ in cyclohexane to give **3** proceeds via the preequilibrium complex **2**. The results are consistent with the

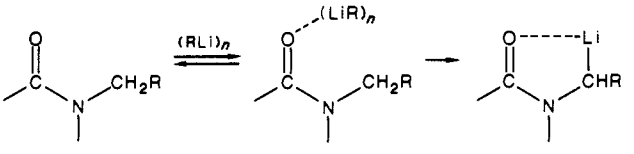

presence of aggregated complexes on the reaction pathway and with the more reactive aggregates having more ligands bound to the lithiums. Interesting features of our data are a decreasing rate of lithiation with increasing *sec*-butyllithium concentration and an effect of tetramethylethylenediamine (TMEDA) consistent with addition of TMEDA and amide substrate to (*s*-BuLi)$_4$ to form aggregated complexes that are reactive.

Results

Kinetics of the α′-Lithiations of 4 and 5. The reactions investigated are the lithiations of *N,N*-dimethyl-2,4,6-triisopropylbenzamide (**4**) and *N,N*-diethyl-2,4,6-triisopropylbenzamide (**5**) by freshly prepared *s*-BuLi in cyclohexane at 25 °C to give the syn α′-lithiated amides **6** and **7**, respectively.[11-14] Kinetic

(1) (a) Gilman, H.; Morton, J. W. *Org. React. (N.Y.)* **1954**, *8*, 258. (b) Gschwend, H. W.; Rodriquez, H. R. *Ibid.* **1979**, *26*. (c) Wakefield, B. J. *The Chemistry of Organolithium Compounds*; Pergamon: Oxford, 1974. (d) Schlosser, M. *Struktur and Reaktivtät Polar Organometalle*; Springer-Verlag: Berlin, 1973. (e) Wardell, J. L. *Comprehensive Organometallic Chemistry*; Wilkinson, F., Stone, G., Abel, E., Eds.; 1982; Vol. 1, Chapter 2. (f) Meyers, A. I. *Acc. Chem. Res.* **1978**, *11*, 375. (g) Beak, P.; Snieckus, V. *Ibid.* **1982**, *10*, 36. (h) Klump, G. W. *Recl. Trav. Chim. Pay-Bas* **1986**, *105*, 1, and references cited therein.

(2) (a) Setzer, W. N.; Schleyer, P. v. R. *Adv. Organomet. Chem.* **1985**, *24*, 353. (b) Klump, G. W.; Geurink, P. J. A.; van Eikema Hommes, N. J. R.; deKanter, F. J. J.; Vos, M. *Recl. Trav. Chim. Pay-Bas* **1986**, *105*, 398.

(3) Fraenkel, G.; Henrichs, M.; Hewitt, M.; Su, B. M. *J. Am. Chem. Soc.* **1984**, *106*, 255. Bauer, W.; Seebach, D. *Helv. Chim. Acta* **1984**, *67*, 1972. Jastrzebski, J. T. B. H.; Van Koten, G.; Konijn, M.; Stam, C. H. *J. Am. Chem. Soc.* **1982**, *104*, 5490.

(4) Kaufmann, E.; Schleyer, P. v. R.; Houk, K. N.; Wu, Y. D. *J. Am. Chem. Soc.* **1985**, *107*, 5560.

(5) Beak, P.; Meyers, A. I. *Acc. Chem. Res.* **1986**, *11*, 356.

(6) Al-Aseer, M. A.; Smith, S. G. *J. Org. Chem.* **1984**, *49*, 2608. Al-Aseer, M. A.; Allison, B. D.; Smith, S. G. *Ibid.* **1985**, *50*, 2715, and references cited therein.

(7) McGarrity, J. F.; Ogle, C. A. *J. Am. Chem. Soc.* **1985**, *107*, 1805. McGarrity, J. F.; Ogle, C. A.; Brich, Z.; Looser, H. R. *Ibid.* **1985**, *107*, 1810.

(8) (a) For cases in polar solvents, see: Holm, T. *Acta. Chem. Scand., Ser. B* **1978**, *B32*, 162. Smith, S. G. *Tetrahedron Lett.* **1966**, 6075. Smith, S. G.; Charbonneau, L. F.; Novak, D. P.; Brown, T. L. *J. Am. Chem. Soc.* **1972**, *94*, 7059. (b) For cases in the presence of complexing agents, see: Collum, D. B. *Ibid.* **1985**, *107*, 2078. Hsieh, H. L. *J. Polym. Sci., Part A-1* **1970**, *8*, 533. Lochman, L.; Lukas, R.; Lim, D. *Collect. Czech. Chem. Commun.* **1972**, *37*, 469. Holm, T. *Acta Chem. Scand.* **1969**, *23*, 1829. Langer, A. W. Advances in Chemistry Series 130; American Chemical Society: Washington, D.C., 1974.

(9) Reich, H. J.; Phillips, N. H.; Reich, I. L. *J. Am. Chem. Soc.* **1985**, *107*, 4101.

(10) Guyot, A.; Vialle, J. *J. Macromol. Sci., Part A-4* **1970**, 79. Roovers, J. E.; Bywater, S. *Macromolecules* **1968**, *1*, 328. Worsford, D. J.; Bywater, S. *Can. J. Chem.* **1964**, *42*, 2884. Mechin, R.; Kaempf, B.; Tanieban, C. *Eur. Polym. J.* **1977**, *13*, 493.

(11) A preliminary account of part of this work has appeared: Al-Aseer, M.; Beak, P.; Hay, D.; Kempf, D. J.; Mills, S.; Smith, S. G. *J. Am. Chem. Soc.* **1983**, *105*, 2080.

(12) Infrared studies of α′-lithioformamidines reached a similar conclusion about the intermediacy of substrate–organolithium complexes: Meyers, A. I.; Fuentes, L. M.; Reiker, W. F. *J. Am. Chem. Soc.* **1983**, *105*, 2082. See also: Fitt, J. J.; Gschwend, H. W. *J. Org. Chem.* **1984**, *49*, 209.

0002-7863/88/1510-8145$01.50/0

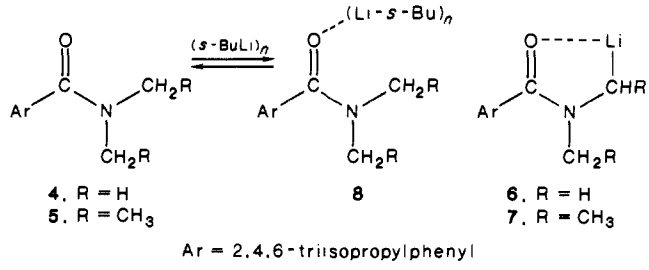

behavior of the infrared bands at 1645–1655 cm^{-1}, due to **4** or **5**, at 1618–1625 cm^{-1}, attributed to intermediate complex(es), and at 1560–1590 cm^{-1}, due to **6** or **7**, was followed by stopped-flow spectroscopy.[6] In all cases, the bands due to the amide and complex(es) were in equilibrium at the shortest observation time of 3 ms and apparent equilibrium constants could be determined.[15] The rate of disappearance of the amide and complex(es) and the rate of appearance of the α'-lithiated product were the same, although the accuracy of data for the low-intensity amide bond was poor and not used for the following analyses. A reaction of **4** carried out in the stopped-flow spectrometer was quenched with D_2O and shown to give the expected product **4**-*d*.[14]

The reaction of **4** with *s*-BuLi in cyclohexane is representative. The reaction was observed over the range (2.58–19.73) × 10^{-3} M in **4** and (2.4–63.0) × 10^{-3} M in tetrameric *s*-BuLi. A plot illustrating the change in percent transmittance of the complex(es) vs time is shown as Figure 1. Treatment of the kinetic data according to a pseudo-first-order rate law of second-order rate law at low concentrations of *s*-BuLi yielded the rate plot shown in Figure 2a. The rate constant determined from the slope of the rate plot increased with increasing time independent of wavelength and slit width suggesting that product-induced catalysis was occurring. Consequently, the rate constants were calculated from the slope of the rate plots for only the initial 10–20% of reaction where the product concentration was low, as shown in Figure 2b. Within experimental error, the observed pseudo-first-order rate constants calculated for the disappearance of the complex and the appearance of the product were identical.

In an attempt to determine the order of the reaction in the reactants, the observed rate constant k_{obsd} was evaluated for the reaction of a constant concentration of 4.84 mM **4** with several concentrations of *s*-BuLi in cyclohexane. In most cases, kinetic data were acquired by measuring the rate of disappearance of the complex band rather than the appearance of the product because of its larger absorbance. Figure 3 shows a plot of k_{obsd} vs *s*-BuLi concentration.[15] The sharp increase in rate at low concentrations of *s*-BuLi and the general shape of the effect suggest the reaction is not of simple order in *s*-BuLi.

In order to determine if the rate-enhancing effect at low *s*-BuLi concentration could be the result of air and consequent alkoxide contamination, the rate constants were measured as a function of the percent lithium alkoxide formed per alkyllithium tetramer after deliberate exposure to air. An effect was found and used to correct all kinetic data on the basis of the small amounts of alkoxide determined to be present by the titrative analysis of the *s*-BuLi reagent we prepared.[15] A small effect of the product catalysis is also noted in Figure 2a. However, even with corrections for these effects (vide infra), the fastest observed rate constant at lowest concentrations is reduced in value by only a modest amount. Although the accuracy of the points at lowest concentrations is the most difficult to measure, even errors that might be substantially larger than what we regard as reasonable would leave the general shape of Figure 3 unchanged.

Measurement of the observed rate constant as a function of the concentration of **4** was carried out to determine the order of the reaction in amide. With a constant initial *s*-BuLi concentration, k_{obsd} increases with increasing **4** as shown in Figure 4.[15]

A stopped-flow infrared spectroscopic study of the reaction of 4.53 × 10^{-3} M **4** with 8.9 × 10^{-2} M *sec*-butyllithium tetramer in the presence of 0–0.212 M tetramethylethylenediamine (TMEDA) in cyclohexane at 25.0 °C was carried out, and the rate of dis-

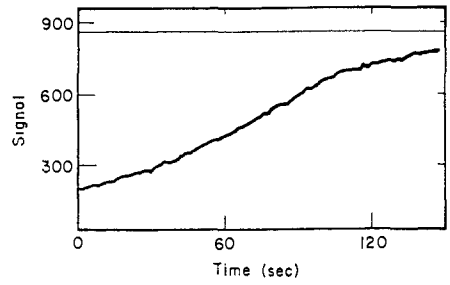

Figure 1. Plot of transmission signal at 1625 cm^{-1} vs time for the reaction of 0.004 53 M *N,N*-dimethyl-2,4,6-triisopropylbenzamide (**4**) with 0.09 M *sec*-butyllithium tetramer in cyclohexane at 25.0 °C. The spectrum was obtained by digitizing 100 data points.

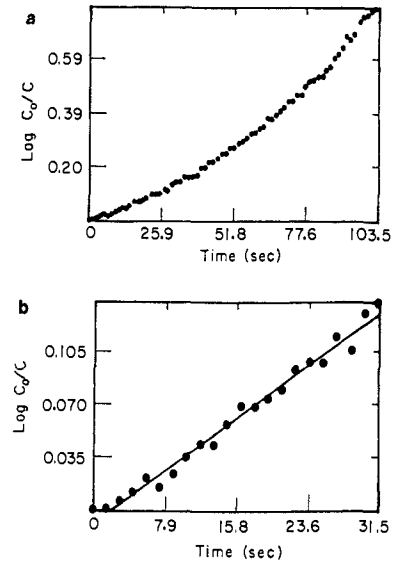

Figure 2. Logarithmic plot of absorbance at infinity divided by absorbance vs time: (a) for the reaction of 0.004 53 M *N,N*-dimethyl-2,4,6-triisopropylbenzamide (**4**) with 0.09 M *sec*-butyllithium tetramer; (b) for the initial 20% of the reaction of 0.004 53 M **4** with 0.09 M *sec*-butyllithium tetramer in cyclohexane at 25.0 °C.

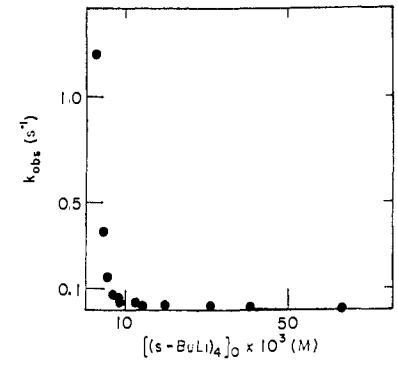

Figure 3. Plot of observed pseudo-first-order rate constant vs concentration of *sec*-butyllithium tetramer upon reaction with 0.004 84 M *N,N*-dimethyl-2,4,6-triisopropylbenzamide (**4**) in cyclohexane as measured at 1625 cm^{-1} and 25.0 °C.

(13) The α'-lithiated amide may be considered a dipole-stabilized carbanion: Beak, P.; Reitz, D. A. *Chem. Rev.* **1978**, *78*, 275. For examples in which related α'-lithiations have particular synthetic value, see: Meyers, A. I.; Diekman, D. A.; Bailey, T. R. *J. Am. Chem. Soc.* **1985**, *107*, 7974. Hoppe, D.; Kramer, T. *Angew. Chem., Int. Ed. Engl.* **1986**, *25*, 160.

(14) For previous work in these and related systems, see: Beak, P.; Zajdel, W. J. *J. Am. Chem. Soc.* **1984**, *106*, 1010. Rondan, N. G.; Houk, K. N.; Beak, P.; Zajdel, W. J.; Chandrasekhar, J.; Schleyer, P. v. R. *J. Org. Chem.* **1981**, *46*, 4316. Seebach, D.; Wykypiel, W.; Lubosch, W.; Kalinowski, H. *Helv. Chim. Acta* **1978**, *61*, 3100. Beak, P.; McKinnie, B. G.; Reitz, D. B. *Tetrahedron Lett.* **1977**, 1839.

(15) Details are available: (a) Hay, D. R. Ph.D. Thesis, University of Illinois, Urbana, IL, 1986. Available from Chemistry Microfilms, Ann Arbor, MI. (b) See supplementary material.

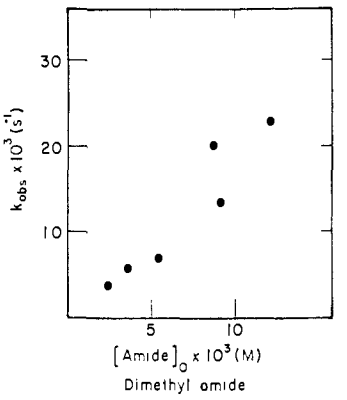

Figure 4. Plot of pseudo-first-order rate constant vs concentration of *N,N*-dimethyl-2,4,6-triisopropylbenzamide (**4**) upon reaction with 0.026 M *sec*-butyllithium tetramer at 25.0 °C.

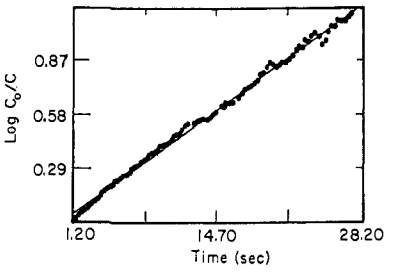

Figure 5. Logarithmic plot of absorbance at infinity divided by absorbance vs time for the reaction of 0.004 53 M *N,N*-dimethyl-2,4,6-triisopropylbenzamide (**4**) with 0.09 M *sec*-butyllithium tetramer catalyzed by 0.042 equiv of TMEDA at 25.0 °C.

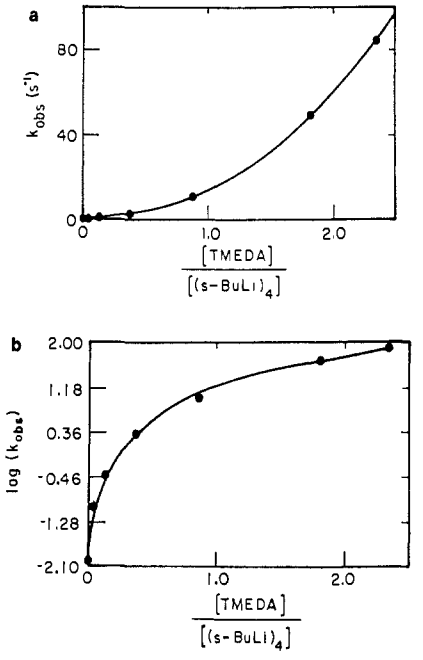

Figure 6. (a) Plot of observed pseudo-first-order rate constant vs concentration of TMEDA divided by 0.09 M *sec*-butyllithium tetramer for the reaction with 0.0045 M *N,N*-dimethyl-2,4,6-triisopropylbenzamide (**4**) in cyclohexane at 25.0 °C as measured at 1625 cm^{-1}. (b) Logarithmic plot of observed pseudo-first-order rate constant vs equivalents of TMEDA.

appearance of the amide complex band was measured. Upon addition of even a small amount of TMEDA, autocatalysis disappears and first-order behavior is seen as shown in Figure 5. The observed rate constant may be calculated as a function of the number of equivalents of TMEDA and plotted as in Figure 6a.[15] Calculation of the logarithm of k_{obsd} against the number of equivalents of TMEDA shows the rate of increase in the observed

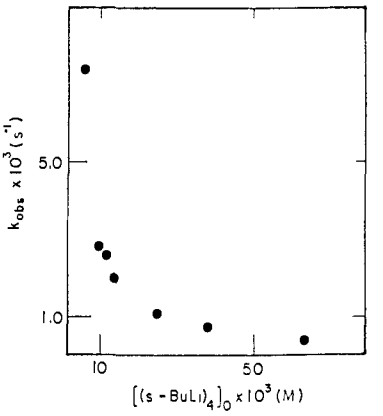

Figure 7. Plot of observed pseudo-first-order rate constant vs concentration of *sec*-butyllithium tetramer upon reaction with 0.0104 M *N,N*-diethyl-2,4,6-triisopropylbenzamide (**5**) in cyclohexane for signal at 1618 cm^{-1} at 25.0 °C.

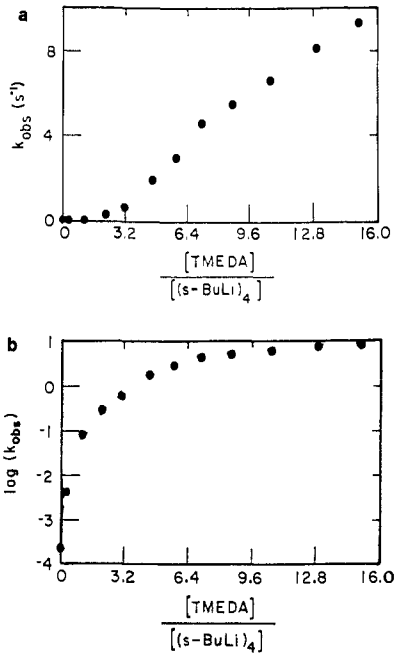

Figure 8. (a) Plot of observed pseudo-first-order rate constant vs equivalents of TMEDA for the reaction of 0.005 24 M *N,N*-diethyl-2,4,6-triisopropylbenzamide (**5**) with 0.0448 M *sec*-butyllithium catalyzed by 0–0.47 M TMEDA. (b) Logarithmic plot of observed pseudo-first-order rate constant vs equivalents of TMEDA at 25.0 °C.

rate constant to be greater at low TMEDA concentrations than at higher levels, as shown in Figure 6b.

The kinetics of the reaction of (4.6–64) × 10^{-3} M *sec*-butyllithium with (3–10.4) × 10^{-3} M *N,N*-diethyl-2,4,6-triisopropylbenzamide (**5**) in cyclohexane at 25.0 °C also were investigated by single-beam stopped-flow infrared spectroscopy. The rate of reaction of **5** was ca. 75 times slower than that of **4**. The pseudo-first-order rate constant, k_{obsd}, vs lithium reagent concentration yielded a curve for **5** similar to that observed for the reaction of **4** with an increase at low alkyllithium concentration, as shown in Figure 7.

The reaction of 5.24 × 10^{-3} M **5** with 4.48 × 10^{-2} M *s*-BuLi in cyclohexane at 25.0 °C catalyzed by 0–0.47 M TMEDA was studied by stopped-flow infrared spectroscopy. The diethylamide **5** is a more appropriate substrate than the dimethylamide **4** for studies with TMEDA because its slower reaction rate allows measurement over a broader range of catalyst concentrations. The kinetics were measured as a function of the number of equivalents of TMEDA, and the data are plotted in Figure 8a. To fully express the catalytic effect of the first few equivalents of TMEDA compared to greater concentrations, the logarithm of the observed

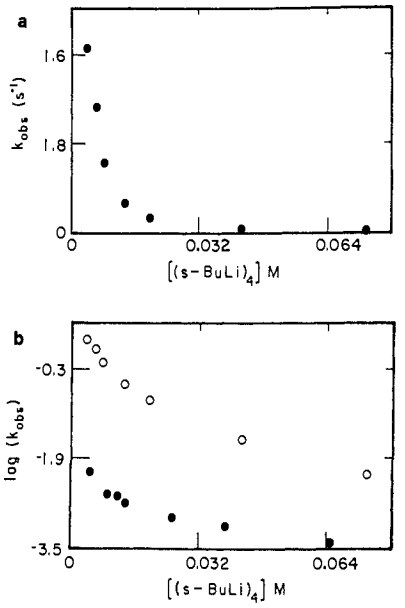

Figure 9. (a) Plot of observed pseudo-first-order rate constant vs concentration of *sec*-butyllithium tetramer for the reaction of 0.00491 M *N,N*-diethyl-2,4,6-triisopropylbenzamide (**5**) with 0–0.08 M *sec*-butyllithium catalyzed by 0.0251 M TMEDA. (b) Logarithmic plot of observed pseudo-first-order rate constant vs *sec*-butyllithium tetramer concentration. The upper points are for the reaction of 0.00491 M **5** catalyzed by 0.0251 M TMEDA. The lower points are for the reaction of 0.0104 M **5** with no TMEDA. The data were measured at 25.0 °C and at a frequency of 1618 cm^{-1}.

rate constant is plotted vs the equivalents of TMEDA per tetrameric *sec*-butyllithium in Figure 8b.

In order to evaluate the effect of changing the concentration of *s*-BuLi in the presence of TMEDA, the kinetics of reaction of 4.9×10^{-3} M *N,N*-diethyl-2,4,6-triisopropylbenzamide (**5**) with (5–68) $\times 10^{-3}$ M *sec*-butyllithium tetramer and 2.51×10^{-2} M TMEDA in cyclohexane at 25.0 °C were measured by stopped-flow infrared spectroscopy. A plot of the observed rate constant measured as a function of the alkyllithium concentration is shown in Figure 9a.[15] The general shape of decreasing rate with increasing *sec*-butyllithium is observed. This is also illustrated by Figure 9 in which the logarithm of the observed rate constants are compared for reaction in the presence and absence of TMEDA.

Complexation between *N,N,N',N'*-Tetramethylethylenediamine and *sec*-Butyllithium in Cyclohexane. A freezing point depression study of mixtures of *s*-BuLi and TMEDA in cyclohexane was undertaken to determine the state of aggregation of the majority of the resulting complex. That information could be useful for interpretation of the kinetics of the above reactions. Measurements were made using a calibrated thermistor enclosed within a hermetically sealed sample tube along with a magnetic stirring mechanism.[15]

With no TMEDA present, the average degree of association of *sec*-butyllithium in cyclohexane near 0 °C was found to 3.46 ± 0.23 suggesting that it exists largely as a tetramer in agreement with previous work.[3,16,17] With TMEDA present, the millimoles of solute calculated as a function of the number of equivalents of TMEDA was determined in four separate experiments. Since these experiments were done with different amounts of reagent, the millimoles of solute and the millimoles of TMEDA were divided by the millimoles of *s*-BuLi used for comparison. A compilation of these results is shown in Figure 10. The curve relates the number of particles formed by the *s*-BuLi–TMEDA complexes as a function of the number of equivalents. Qualitatively, disassociation to smaller species would lead to a rapid increase in the number of equivalents of solute. That behavior is not observed, and apparently the *s*-BuLi remains largely associated in the presence of TMEDA with TMEDA simply associating with the tetramer.

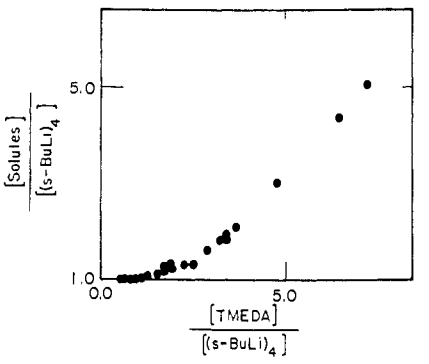

Figure 10. Plot of the number of millimoles of solute per millimoles of *sec*-butyllithium tetramer vs the equivalents of TMEDA per *sec*-butyllithium tetramer as determined by the freezing point depression in cyclohexane.

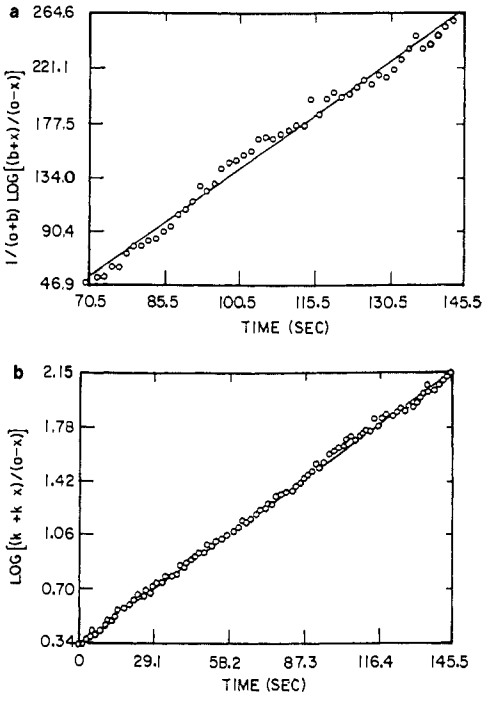

Figure 11. (a) Logarithmic plot of second-order autocatalytic rate law for the latter 50% of the reaction of 0.00453 M *N,N*-dimethyl-2,4,6-triisopropylbenzamide (**4**) with 0.09 M *sec*-butyllithium tetramer. (b) Logarithmic plot of the first-order part of the two-term rate law derived from second-order autocatalysis for the reaction of 0.00453 M **4** with 0.09 M *sec*-butyllithium tetramer in cyclohexane at 25.0 °C.

Discussion

Regardless of any interpretation of this data, the decreasing rates of lithiation of **4** and **5** with increasing concentrations of *s*-BuLi are of interest. In our own efforts to induce reluctant lithiations to proceed, we often use an excess of the organolithium reagent; the trends shown in Figures 3, 7, and 9 can be taken to suggest such attempts may sometimes be counterproductive. It should be noted the present reactions are studied in hydrocarbon solvent and might be suitable for discussion of reactions with "unsolvated" organolithium reagents, but since most lithiations are carried out in ether solvents, extension of these observations to such conditions is problematic.

Before the kinetic data can be analyzed, it must be corrected for the effects of autocatalysis and of alkoxide impurities on the reaction rates. The autocatalysis that is indicated by the curve of Figure 2 was found to exist over a wide range of lithium reagent

(16) Bywater, W.; Worsford, D. J. *J. Organomet. Chem.* **1967**, *10*, 1. Allison, B. D., Ph.D. Thesis, University of Illinois, Urbana, IL, 1978.

(17) We examined the change in proton magnetic resonance of *sec*-butyllithium as a function of TMEDA and observed a change in chemical shift of the α-proton which levels off at 3 equiv of TMEDA and is consistent with the freezing point depression data.[3,15]

and amide concentrations. Treatment of this effect in a two-term rate expansion as a simple second-order catalytic reaction in which the product **6** catalyzes the reaction of the amide **5** with *s*-BuLi provides an autocatalytic rate constant (see the supplementary material). Thus, the first- and second-order parts of the reaction can be separated. Removal of this effect of autocatalysis provided minor correction and gives the values for the first-order part of the reaction shown in Figure 11.[15,18]

The autocatalysis observed in Figure 2 may be taken to provide a clue to the structure of the reagent as well as the mechanism by which it reacts. A straightforward explanation of autocatalysis is that the lithiated amide product remains associated within an aggregate that still has active *s*-BuLi and can react in the lithiation of a second amide molecule. In this aggregate, the *s*-BuLi acts as a reagent of somewhat higher reactivity than in its initial tetrameric form.

It is known that alkoxides can provide significant rate enhancements in reactions of organolithium substrates. Although our reactions were carried out with freshly prepared *s*-BuLi, with vacuum line techniques, and under inert atmospheres, contamination by air and formation of rate-enhancing species is conceivable. Deliberate admission of air, titration of alkoxide formed, and kinetic analysis of the rates of reaction of the resulting reagent provided a correction curve that could be used to calculate the observed rate constant free from alkoxide contamination.[15] The correction values were small, and treatment of the data of Figure 2 in this way provided only slightly different values. It should be noted again that the present analysis is based on the corrected *initial rate constants* and applies to that portion of the reaction.

The simplest version of a complex-induced proximity effect in directing the α′-lithiations of the amides **4** or **5** is illustrated in Scheme I. Reaction of *s*-BuLi with the amide **4** or **5** to give the complex[8] would be followed by removal of a proton by the *s*-Bu group and formation of the α′-lithiated product **6** or **7**. Under this scheme, the reaction would be first or fractional order in *s*-BuLi depending on the aggregation of the reactive organolithium species involved in the complex. The reaction also would be first order in amide, and the reaction would have a single-valued equilibrium constant for the initial association. However, the data do not fit these expectations. The decrease in rate with increasing *s*-BuLi at low *s*-BuLi concentrations shown in Figures 3, 7, and 9 is an especially clear illustration of the inadequacy of Scheme I.

Scheme I

$$\text{amide} + (s\text{-BuLi})_4 \overset{K_1}{\rightleftharpoons} \text{amide}\cdot(s\text{-BuLi})_4 \xrightarrow{k} \text{products}$$

We have carried out computer simulation analyses of a number of possible kinetic schemes and have not been able, within the constraints of this system, to construct a single scheme that provides a quantitative and unique fit to all of our data. However, we can consider several simple schemes to determine whether they appear to adequately model our observations. The schemes that were analyzed are progressively more complicated and are presented so the extent of the analysis is clear. While the complexity of the possible mechanisms are such that we cannot be certain we have considered all ramifications of each possibility, we believe the present analysis to be illuminating. We do not claim the fit of the schemes that we prefer to be unique, only that we have been unable to obtain even approximately satisfactory fits with simpler Schemes II–V. The attempted fits of the assumptions of Schemes II–V to the data are available.[15]

Any mechanistic scheme of first or higher order in lithium reagent concentration that we have tested does not fit the data. The fact that the rate must rise rapidly and then drop almost as rapidly with increasing lithium reagent concentration argues for a mechanism involving at least two processes. Similar kinetic behavior was observed by Al-Aseer and Smith for the addition of *s*-BuLi to esters in cyclohexane.[6] Adaptation of their scheme to the present case provides Scheme II. According to this scheme, the rate constant is regulated by the tetramer–monomer equilibrium. The initial portion of the curve at very low reagent concentration is essentially first order in monomer, but as the total alkyllithium concentration increases, the concentration of the tetramer increases rapidly due to the fourth-order dependence defined by the equilibrium. The tetramer binds the substrate in a relatively unreactive complex, and the observed rate constant consequently decreases with increasing *s*-BuLi.

Scheme II

$$(s\text{-BuLi})_4 \overset{K_1}{\rightleftharpoons} 4(s\text{-BuLi})_1$$

$$(s\text{-BuLi})_4 + \text{amide} \overset{K_2}{\rightleftharpoons} \text{amide}\cdot(s\text{-BuLi})_4$$

$$\text{amide}\cdot(s\text{-BuLi})_4 \xrightarrow{k_3} \text{product}$$

$$(s\text{-BuLi})_1 + \text{amide} \xrightarrow{k_4} \text{product}$$

$$K_1 = 10^{-7};\ K_2 = 10^4;\ k_3 = 0,\ k_4 = 6 \times 10^2$$

Computer simulations using this mechanism were undertaken for comparison with the data in Figures 3 and 4. By use of the dissociation equilibrium constant reported in the literature, values of K_2, k_3, and k_4 were estimated as necessary to provide the best possible fit and as shown in Scheme II. While the basic shape of the Figure 3 curve was reproduced, the fit was poor.[15b] Furthermore, the rate constant exhibits only a moderate dependence on the amide concentration regardless of the reagent concentration, and therefore, this scheme does not provide a fit to Figure 4.

It has been suggested that dimers are the reactive species in metalations of this type.[7] If one modifies the above scheme to employ dimers instead of monomers, the computer simulation shows the general inverse relationship between rate constant and reagent concentration can again be reproduced. However, the fit to Figure 3 is even poorer.[15a]

If Scheme II is modified to incorporate a monomeric complex in addition to the tetrameric complex, as in Scheme III, an increase in the lithium reagent could distort the tetramer–monomer equilibrium sufficiently such that the observed rate constant might fit the kinetic data. Again the best fit to the data was found by computer simulation with the values shown in the scheme. This did result in a reasonable fit to Figure 3 but showed poor sensitivity to changes in the amide concentration, which is not consistent with the data in Figure 4.[15b]

Scheme III

$$(s\text{-BuLi})_4 \overset{K_1}{\rightleftharpoons} 4(s\text{-BuLi})_1$$

$$(s\text{-BuLi})_4 + \text{amide} \overset{K_2}{\rightleftharpoons} \text{amide}\cdot(s\text{-BuLi})_4$$

$$(s\text{-BuLi})_1 + \text{amide} \overset{K_3}{\rightleftharpoons} \text{amide}\cdot(s\text{-BuLi})_1$$

$$(s\text{-BuLi})_4\,\text{amide} \xrightarrow{k_4} \text{product}$$

$$(s\text{-BuLi})_1\,\text{amide} \xrightarrow{k_5} \text{product}$$

$$K_1 = 10^{-7};\ K_2 = 10^7;\ K_3 = 10^5;\ k_4 = 10^{-3};\ k_5 = 1$$

Scheme III then was altered to include a term in which the tetrameric complex can react with a second amide molecule to give the product as in Scheme IV. This would incorporate the amide concentration directly into the rate law. Computer modeling did indeed show the correct general curve shapes both as a function of *s*-BuLi concentration and as a function of amide concentration. Surprisingly, however, it did so when the contribution of the monomer was completely ignored by assigning $K_1 = K_3 = k_5 = 0$. Furthermore, the equilibrium constant for tetrameric complex formation must be very large to accomplish this fit and that is not consistent with the measured absorbance data. However, this

(18) Moore, J. W.; Pearson, R. G. *Kinetics and Mechanism*; Wiley: New York, 1981.

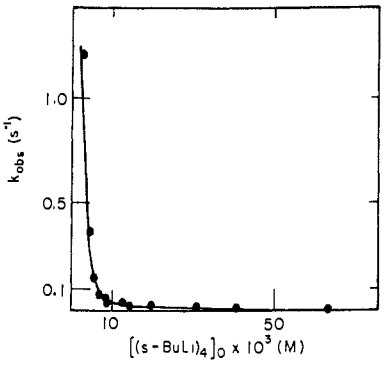

Figure 12. Comparison of Scheme VI to the experimental data for the lithiation of **4** with the values of Scheme VI.

scheme does provide a useful point of departure to explore other possible mechanisms.

Scheme IV

$$(s\text{-BuLi})_4 \overset{K_1}{\rightleftharpoons} 4(s\text{-BuLi})_1$$

$$(s\text{-BuLi})_4 + \text{amide} \overset{K_2}{\rightleftharpoons} \text{amide}\cdot(s\text{-BuLi})_4 \xrightarrow{k_4} \text{product}$$

$$(s\text{-BuLi})_1 + \text{amide} \overset{K_3}{\rightleftharpoons} \text{amide}\cdot(s\text{-BuLi})_1 \xrightarrow{k_5} \text{product}$$

$$(s\text{-BuLi})_4\text{amide} + \text{amide} \xrightarrow{k_6} \text{product}$$

$K_1 = 0$; $K_2 = 10^4$; $K_3 = 0$; $k_4 = 0$; $k_5 = 0$; $k_6 = 1.2 \times 10^2$

Scheme IV was elaborated to incorporate a second equilibrium. The formation of a new complex, $\text{amide}_2\cdot(s\text{-BuLi})_4$, and an additional product formation step was proposed as shown in Scheme V. Competition between the two complexes and introduction of the amide concentration directly into the rate law provided a better fit to the data of Figure 4 with the values shown but failed to fit Figure 3.[15b]

Scheme V

$$(s\text{-BuLi})_4 + \text{amide} \overset{K_1}{\rightleftharpoons} \text{amide}\cdot(s\text{-BuLi})_4 \xrightarrow{k_3} \text{product}$$

$$\text{amide}\cdot(s\text{-BuLi})_4 + \text{amide} \overset{K_2}{\rightleftharpoons} \text{amide}_2\cdot(s\text{-BuLi})_4 \xrightarrow{k_4} \text{product}$$

$K_1 = 10^3$; $K_2 = 5 \times 10^2$; $k_3 = 3 \times 10^{-3}$; $k_4 = 10^{-1}$

Thus, Scheme V was further expanded to include another complex, $\text{amide}_3\cdot(s\text{-BuLi})_4$, which can react to yield product as shown in Scheme VI. Solving the equations for this scheme results in a reasonable fit to all the data.

Scheme VI

$$(s\text{-BuLi})_4 + \text{amide} \overset{K_1}{\rightleftharpoons} (s\text{-BuLi})_4\text{amide} \xrightarrow{k_4} \text{product}$$

$$\text{amide}\cdot(s\text{-BuLi})_4 + \text{amide} \overset{K_2}{\rightleftharpoons} \text{amide}_2\cdot(s\text{-BuLi})_4 \xrightarrow{k_5} \text{product}$$

$$\text{amide}_2\cdot(s\text{-BuLi})_4 + \text{amide} \overset{K_3}{\rightleftharpoons} \text{amide}_3\cdot(s\text{-BuLi})_4 \xrightarrow{k_6} \text{product}$$

$K_1 = 2 \times 10^3$; $K_2 = 2 \times 10^2$; $K_3 = 5 \times 10$; $k_4 = 10^{-3}$; $k_5 = 2 \times 10^{-1}$; $k_6 = 1.5 \times 10$

Scheme VI is then the result of our modeling of the reaction of *N,N*-dimethyl-2,4,6-triisopropylbenzamide (**4**) in cyclohexane at 25 °C with *s*-BuLi to give the α'-lithiated amide **6**.[15,19] In this scheme, free amide and tetrameric *s*-BuLi are in equilibrium with at least three complexes which differ in the number of amides associated with the tetramer. Each of the complexes give the α'-lithiated amide **6** at different rates. The values of equilibrium and rate constants shown in Scheme VI provide fits to the experimental data of Figures 3 and 4 which are shown in Figures 12 and 13. In addition, Scheme VI can be used to provide an estimate of equilibrium between free and complexed amide which provide a reasonable fit to the experimental data.[15b] Although the fits are not exact, we have been unable to find any simpler model that even provides comparable curve shapes.

(19) For simplicity, the product **6** is written as a monomeric species, although it surely remains associated consistent with its effect in autocatalysis.

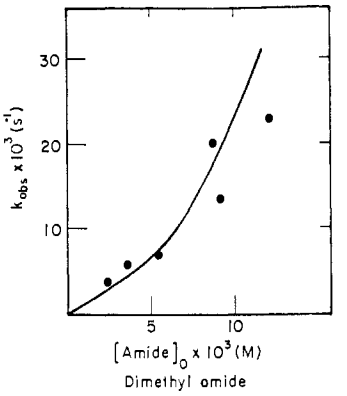

Figure 13. Comparison of Scheme VI for **4** to the experimental data.

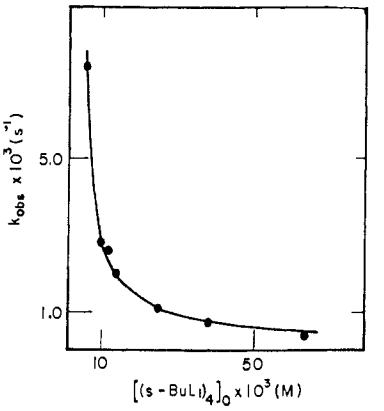

Figure 14. Extrapolation of Scheme VI to the experimental data for the lithiation of **5** with $K_1 = 5 \times 10^2$, $K_2 = 5 \times 10^2$, $K_3 = 1$, $k_1 = 0$, $k_2 = 2 \times 10^{-3}$, and $k_3 = 1$.

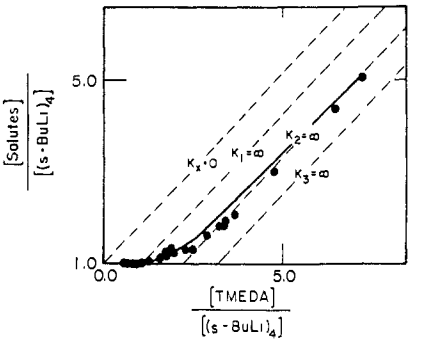

Figure 15. Data of Figure 10 with values of K from Scheme VII.

Application of an analogous scheme to the reaction of *N,N*-diethyl-2,4,6-triisopropylbenzamide (**5**) with *s*-BuLi tetramer to provide **7** with $K_1 = 5 \times 10^2$, $K_2 = 5 \times 10^2$, $K_3 = 1$, $k_1 = 0$, $k_2 = 2 \times 10^{-3}$, and $k_3 = 1$ also provides a satisfactory fit to the experimental data as shown in Figure 14. These schemes are complex, and we emphasize that while we have not been able to find simpler alternatives that provide a fit to the data by the approach we have described above, alternatives of comparable and greater complexity surely exist that also would provide a fit.

The α'-lithiations of **4** and **5** with *s*-BuLi in the presence of TMEDA appear to be even more complex. The freezing point depression data summarized in Figure 10 show that TMEDA does not break up the tetrameric *s*-BuLi in a macroscopically detectable way under the conditions used in this study. The same number

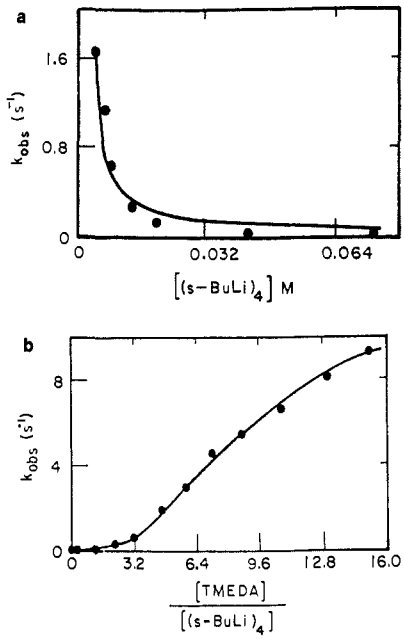

Figure 16. Comparison of Scheme VIII to the experimental data for the lithiation of **5** with *s*-BuLi–TMEDA.

of millimoles of solute are present in solution when 1 equiv of TMEDA is present as when none is added. This suggests the first complex exists largely as TMEDA·(*s*-BuLi)$_4$. As more TMEDA is added, the millimoles of solute increase slowly, consistent with the formation of TMEDA$_2$·(*s*-BuLi)$_4$, after which the curve rises linearly with a slope of 1 indicating little additional complexation.

In order to delineate which TMEDA-complexed species might be present in solution and their relative abundances, limits were calculated and imposed on the data according to the possible equilibria proposed in Scheme VII.

Scheme VII

$$4\text{TMEDA} + (sec\text{-BuLi})_4 \overset{K_0}{\rightleftharpoons} 4\text{TMEDA}\cdot(sec\text{-BuLi})_1$$

$$\text{TMEDA} + (sec\text{-BuLi})_4 \overset{K_1}{\rightleftharpoons} \text{TMEDA}\cdot(sec\text{-BuLi})_4$$

$$\text{TMEDA} + \text{TMEDA}\,(sec\text{-BuLi})_4 \overset{K_2}{\rightleftharpoons} (\text{TMEDA})_2\cdot(sec\text{-BuLi})_4$$

$$\text{TMEDA} + (\text{TMEDA})_2\cdot(sec\text{-BuLi})_4 \overset{K_3}{\rightleftharpoons} (\text{TMEDA})_3\cdot(sec\text{-BuLi})_4$$

$$K_0 = 0;\ K_1 = 10^3;\ K_2 = 10^2;\ K_3 = 0$$

The scheme can be understood by considering its limits. If there was no association, all of the equilibrium constants would be zero, and addition of TMEDA would simply increase the millimoles of solute linearly and with a slope of 1. This is illustrated by the limiting line designated $K_x = 0$ in Figure 15. The other limits for each equation occur when the equilibrium constant for one term is infinite and the others are zero thereby defining the boundaries within which the data would be expected to fall for any given equation of the proposed scheme. These infinity limits are illustrated in Figure 15 as dotted lines. Consistent with expectation, complexes between tetrameric *s*-BuLi and 1 or 2 equiv of TMEDA appear to be present.[1,2] Values of $K_1 = 10^3$, $K_2 = 10^2$, and $K_3 = 0$ with $K_0 = 0$ provide the fit shown in Figure 15. It is not, of course, necessary that the major species in solution be the active species along a reaction pathway. The well-known effect of TMEDA in accelerating lithiation reactions is usually rationalized in terms of TMEDA promoting the formation of less aggregated more reactive complexes, although that explanation has been questioned.[1,2,8]

The rates of α′-lithiation of **5** in the absence and presence of TMEDA are shown in Figures 7 and 9a. These curves show the same general decreases of rate with increasing *s*-BuLi concentration as discussed above. Comparison of the two curves in Figure 9b shows a 10 to 10^2 rate acceleration attributable to the presence of TMEDA. We determined that in the presence of TMEDA the autocatalysis and alkoxide catalysis effects are negligible. It is clear that a scheme analogous to Scheme I including a reactive TMEDA·(*s*-BuLi)$_1$ complex will not fit these experimental observations. Figure 8a shows the dependence of the rate constant as a function of the number of equivalents of TMEDA. The true effect, however, becomes clearer when the logarithm of k_{obsd} is calculated as in Figure 8b. The most rapid change in rate occurs at the low levels of catalyst concentration.

Computer simulation was again used to find a scheme that would approximate the data. That is shown as Scheme VIII with the values that provide the fit to the experimental data shown in Figure 16.[15] Although the scheme is complex, the associations involved are well precedented and the equilibria are sensible and consistent with expectation.[1-8] Application of a similar scheme to **4** with $K_1 = 2 \times 10^3$, $K_2 = 2 \times 10^2$, $K_3 = 10^3$, $K_4 = 10^2$, $K_5 = 10^4$, $K_6 = 10$, $K_7 = 10$, $k_1 = 0$, $k_2 = 5 \times 10$, and $k_3 = 5 \times 10^3$ also gives a satisfactory fit to the data for that reaction.[15b]

Scheme VIII

$$\mathbf{5} + (s\text{-BuLi})_4 \overset{K_1}{\rightleftharpoons} \mathbf{5}\cdot(s\text{-BuLi})_4$$

$$\mathbf{5} + \mathbf{5}\cdot(s\text{-BuLi})_4 \overset{K_2}{\rightleftharpoons} \mathbf{5}_2\cdot(s\text{-BuLi})_4$$

$$\text{TMEDA} + (s\text{-BuLi})_4 \overset{K_3}{\rightleftharpoons} \text{TMEDA}\cdot(s\text{-BuLi})_4$$

$$\text{TMEDA} + \text{TMEDA}\cdot(s\text{-BuLi})_4 \overset{K_4}{\rightleftharpoons} (\text{TMEDA})_2\cdot(s\text{-BuLi})_4$$

$$\mathbf{5} + \text{TMEDA}\cdot(s\text{-BuLi})_4 \overset{K_5}{\rightleftharpoons} \mathbf{5}\cdot\text{TMEDA}\cdot(s\text{-BuLi})_4$$

$$\mathbf{5} + \mathbf{5}\cdot\text{TMEDA}\cdot(s\text{-BuLi})_4 \overset{K_6}{\rightleftharpoons} \mathbf{5}_2\cdot\text{TMEDA}\cdot(s\text{-BuLi})_4$$

$$\mathbf{5} + (\text{TMEDA})_2\cdot(s\text{-BuLi})_4 \overset{K_7}{\rightleftharpoons} \mathbf{5}\cdot(\text{TMEDA})_2\cdot(s\text{-BuLi})_4$$

$$\mathbf{5}\cdot\text{TMEDA}\cdot(s\text{-BuLi})_4 \xrightarrow{k_1} \mathbf{7}$$

$$\mathbf{5}_2\cdot\text{TMEDA}\cdot(s\text{-BuLi})_4 \xrightarrow{k_2} \mathbf{7}$$

$$\mathbf{5}\cdot(\text{TMEDA})_2\cdot(s\text{-BuLi})_4 \xrightarrow{k_3} \mathbf{7}$$

$K_1 = 5 \times 10^2$; $K_2 = 5 \times 10^2$; $K_3 = 10^3$; $K_4 = 10^2$; $K_5 = 10^4$; $K_6 = 10$; $K_7 = 10$; $k_1 = 0$; $k_2 = 5$; $k_3 = 5.3 \times 10$

While we can conclude that the present data cannot be fit by schemes that involve reaction of one kind of complex or dissociated species, we stress that these schemes may not be unique and interpretation of these results is best made on a semiquantitative basis. The reactions shown in Schemes VI and VIII do illustrate the difficulties in suggesting detailed reaction pathways for the reactions of organolithium compounds. There are different equilibrium constants for the formations of different reactive complexes, and these complexes exhibit different reactivities. The major species in solution may not be on the reaction pathway, and the extent of reaction by different pathways can change as a function of the reaction conditions.[2,20] The decreasing rates of lithiation with increasing *s*-BuLi concentration observed in hydrocarbon solvent seem contradictory to reasonable intuition,

(20) In doing competitive studies to assess relative reactions, the usual measure of carrying out reactions under identical conditions may not resolve the problem since different curve shapes could be observed with different reactants. Autocatalysis, which could be different for different substrates, could also affect the results. The complexity of these schemes may also account for diversity sometimes encountered in comparing results from different laboratories. Empirical studies, perhaps over wider ranges than considered heretofore, appear still to be needed in each case. For example, the present results suggest that some lithiation reactions would proceed faster in the presence of less organolithium substrate and that higher aggregates of organolithium species may be more reactive than lower aggregates in some cases.

although this effect is precedented in other reactions of organolithium reagents.[6]

The fact of acceleration of reactions of organolithium reagents by additions of complexing agents has been long recognized.[1-8] The observation of autocatalysis in this case also illustrates the fact that ligands on the organolithium reagent can affect its reactivity. If the reaction occurred exclusively between the substrate and a monomeric reagent molecule, the product concentration would not be expected to have an influence on the rate.

It is interesting that under the present analysis the complexes become more reactive as they are bound to more ligands. In Scheme VI, the first equivalent of amide is tightly bound but the complex is not very reactive. The second equivalent is less strongly bound but the complex is much more reactive, and the third equivalent makes the complex more reactive than the second. Under Scheme VIII, the complex of *s*-BuLi tetramer with one amide and one TMEDA is not converted to product at a competitive rate. The most reactive complexes are those that have one or two amides and one or two TMEDA ligands associated in the reactive aggregate, with the latter much more reactive.

We suggest that in the most reactive complexes one lithium is bound to the oxygen of the carbonyl group and the other lithiums are also bound to ligands. The key step may be envisioned then to involve a transition structure in which the reactive *sec*-butyl group is being released from its associated lithiums by their binding to other ligands. Under this hypothesis, the effect of the amide and of TMEDA as an accelerant for the reaction is derived from the abilities of these ligands to bind the lithium atoms in the reactive complex so that the reactive organic moiety becomes available for reaction. This is illustrated for **8** in which the

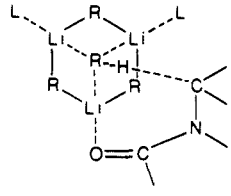

8: R = *s*-Bu, L = complexing ligand

sec-butyl group is being released from the tetramer to remove the α'-proton from the amide by binding of that lithium to the amide and to ligands L. In order to rationalize the order of relative rates of reaction of the complexes in Scheme VIII under this suggestion, we have to claim that the unreactive complex that has one amide and one TMEDA on tetrameric *s*-BuLi has the second site of TMEDA binding to the lithium largely diagonal to the reactive *sec*-butyl group in the complex.

The role of complexing agents and aggregation on the reactions of organolithium species has been discussed often. In summarizing the earlier literature, Langer and Wakefield have suggested that reactions occur in complexed aggregates, and they as well as others have noted this effect could be demonstrated in a variety of ways.[1-8,21] In particular, McGarrity recently provided evidence for increased reactivity of butyllithium in aggregates bearing alkoxides.[7] The present suggestion that the role of TMEDA is to provide complexation in the transition structure can be regarded as an alternative to the suggestion that TMEDA makes an organolithium more reactive by breaking down the aggregated structure to monomers. Perhaps the reason the TMEDA makes an organolithium "more basic" is that the association raises the energy of transition structures for alternative reactions.

The above analyses of the kinetics of α'-lithiations of the amides **4** and **5** by *sec*-butyllithium in both the presence and absence of TMEDA suggest these reactions to be complex, but the hypothesis about the transition structure that emerges from this analysis is straightforward. Our observations are consistent with reaction of aggregates and activation within complexes of aggregates by association of the lithiums that are bound to the reactive group with other ligands. Similar models could rationalize the accelerating effect of ligands on reactions of organolithium substrates under other conditions, although it is again to be noted the present work is done in cyclohexane. The interplays of these possible effects with the effect of concentration, temperature, and different solvents are issues for future work.

(21) This suggestion is also compatible with work that shows TMEDA favorably associates with organolithium substrates and questions if its sole effect is that of producing reactive monomers.[1,2b] For example, McKeever et al. have shown that tetrameric methyllithium maintains its association in TMEDA: McKeever, L. D.; Waack, R.; Doran, M. A.; Baker, E. B. *J. Am. Chem. Soc.* **1969**, *91*, 1057.

Experimental Section

***N*,*N*-Dimethyl-2,4,6-triisopropylbenzamide (4) and *N*,*N*-diethyl-2,4,6-triisopropylbenzamide (5)** were prepared as described.[13,22]

***sec*-Butyllithium.** Solutions of the lithium reagent were prepared in an all-glass, grease-free vacuum line under a blanketing atmosphere of argon. The apparatus was repeatedly evacuated to less than 1 Torr with a high-capacity pump and filled with argon (Linde, passed through a BTS catalyst column to remove oxygen and through 4A molecular sieves to remove water) to ensure proper reaction conditions. Cyclohexane from Aldrich Chemical Co. was dried by refluxing over *sec*-butyllithium in the solvent stills.

The lithium was obtained as an ingot from Lithcoa and cut into chips under mineral oil. It was washed several times with hexane and then transferred to the reaction flask as a slurry after which the solvent was removed by high argon pressure through a sintered glass filter. An addition flask containing *sec*-butyl chloride (Aldrich) freshly distilled from phosphorus pentoxide was attached to the reaction flask and degassed by 2 or 3 freeze–thaw cycles. Cyclohexane was distilled onto the lithium, and the *sec*-butyl chloride was added over a period of ~30 min at 0 °C with stirring. The resulting *sec*-butyllithium solution was allowed to stir for an additional 30 min and then settle for ~4 h. The clear, colorless supernatant was filtered three times through sintered glass and pushed into septum-capped bottles by high argon pressure. Concentrations were varied by distilling additional solvent into the bottles to the desired level.

The lithium reagents were analyzed by Gilman double titration for total base and weak base titers. The total base titer was determined by quenching an aliquot of the reagent with 95% ethanol and titrating with standard hydrochloric acid to a methyl red indicator endpoint. The weak base concentration resulting from air oxidation of the reagent to yield lithium *sec*-butoxide was determined by injecting an excess of 1,2-dibromoethane into the reagent bottle to neutralize the alkyllithium. Aliquots of the resulting solutions were quenched with aqueous ethanol and titrated with standard hydrochloric acid, as before. The alkoxide concentration varied widely from 0.5% to 20% with increasing proportions occurring as the total base concentration decreased. The active *sec*-butyllithium concentration was calculated by subtracting the weak base from the total base concentration.

Kinetic Measurements and Data Analysis. Kinetic experiments were performed with a single-beam stopped-flow infrared spectrometer designed and built at the University of Illinois. Drive and stop syringes were operated with a 1-hp Delta Power Hydraulic Co. pump and a control panel designed and built at the University of Illinois. The spectrometer used a Jarrell–Ash monochromator connected to a synchronous stepping motor for rapid-scanning purposes. The infrared source was a Sylvania C100 arc lamp held within a water-cooled housing under argon. The detector was a cadmium telluride photocell cooled to 77 K with liquid nitrogen which rendered a millivolt signal proportional to the light transmitted through the observation cell. This signal was amplified and digitized with instruments designed and built at the electronics shop of the University of Illinois. Data processing and storage were performed with a PLATO V computer, designed at the University of Illinois, using the microtutor computer language.

Infrared spectra were obtained by digitizing 384 transmittance measurements at the desired time intervals under rapid-scanning conditions. Spectra of reacting solutions were performed under continuous flow conditions. The data were collected, averaged, and stored on floppy disks. To compensate for the cyclohexane spectrum unavoidably included with all spectra on a single-beam spectrometer, its spectrum was measured independently and subtracted by computer from the spectrum of interest under identical conditions. This yielded the desired absorbance spectrum, which could then be readily compared with other spectra obtained in the same manner.

Determination of the free amide concentration upon complexation was performed by measuring the amide carbonyl absorbance at known concentration before mixing to calculate the extinction coefficient. After being mixed with the *sec*-butyllithium reagent under continuous flow conditions, the free amide absorbance was measured as in Figure 3 and

(22) Fuson, R. C.; Horning, E. C. *J. Am. Chem. Soc.* **1940**, *62*, 2962.

averaged. The concentration of the free amide remaining after complexation could then be calculated from the extinction coefficient and used to determine the apparent equilibrium constant. The equilibrium between free amide and the *sec*-butyllithium–amide complex was established within less than ca. 3 ms, which is the time required for the flowing solutions to move from the mixer to the observation chamber.

Kinetic data were obtained by digitizing 100 transmittance measurements at a specified wavelength and time interval under rapid stopped-flow conditions. Plots of percent transmittance vs time were generated via computer using measured zero and infinity light readings. The data were stored and then processed according to whether the absorbance increased or decreased and to the appropriate rate law. Unweighted linear regression analysis of the treated data versus time yielded the pseudo-first-order rate constants which were typically reproducible within 5%.

Freezing Point Depression Measurements and Data Analysis. The thermistor tube was hermetically sealed with a septum and connected to a vacuum line via a 2-ft stainless steel needle. Inside the tube was a glass stirring rod to which was attached a magnet and a 100-kΩ thermistor. Two wire leads connected to the thermistor were threaded through the septum and connected to the Wheatstone bridge. As the temperature of the environment about the thermistor changes, its resistance changes in a nearly linear fashion within a certain temperature range. A Wheatstone bridge transforms this change in resistance into a voltage change which is amplified, digitized, and recorded on a PLATO V computer using the same system as described in the previous section.

The thermistor was calibrated by immersing it in an ethanol–water/dry ice bath along with a precision calibrated thermometer from the National Bureau of Standards graduated in tenths of a degree Celsius. The digitized signal was measured as a function of temperature over the range of −5 to +7 °C, and all subsequent signal readings were transformed into temperatures with this calibration curve.

Cyclohexane was introduced into the thermistor tube with the aid of a gas-tight calibrated syringe. It was then chilled and agitated by moving an external magnet up and down adjacent to the internal magnete. The temperature was measured as a function of time, giving an initial endotherm and supercooling, followed by an exotherm resulting from the heat of crystallization, followed by a plateau. Extrapolating the plateau back to the endotherm gives the temperature of the freezing point. Changes in freezing point depression and observable precipitation did occur after ~30 min, so these experiments were carried out for no longer than 20 min.

Computer Modeling. The fitting of a model to the data was done by deriving equations from the rate and equilibrium expressions defined by the scheme being tested. The initial concentrations of the reagent, substrate, and catalyst employed in the experiment being modeled were used in these equations and the results compared to the experimental observations.

Acknowledgment. We are grateful to the donors of the Petroleum Research Fund, administered by the American Chemical Society, and the National Science Foundation for support.

Registry No. 4, 57199-01-6; **5**, 64712-52-3; *sec*-butyllithium, 598-30-1.

Supplementary Material Available: Tables, figures, and discussion of kinetic data for reactions of **4** and **5**, freezing point depressions, and general analyses of Schemes VI and VIII (28 pages). Ordering information is given on any current masthead page.

Asymmetric Synthesis Catalyzed by Chiral Ferrocenylphosphine–Transition-Metal Complexes. 6.[1] Practical Asymmetric Synthesis of 1,1′-Binaphthyls via Asymmetric Cross-Coupling with a Chiral [(Alkoxyalkyl)ferrocenyl]monophosphine/Nickel Catalyst

Tamio Hayashi,* Keiichi Hayashizaki, Takao Kiyoi, and Yoshihiko Ito*

Contribution from the Department of Synthetic Chemistry, Faculty of Engineering, Kyoto University, Kyoto 606, Japan. *Received March 28, 1988*

Abstract: Cross-coupling of (2-methyl-1-naphthyl)magnesium bromide (**1a**) with 2-methyl-1-naphthyl bromide (**2a**) at −15 or 0 °C in the presence of nickel catalyst prepared in situ from nickel bromide and (*S*)-1-[(*R*)-2-(diphenylphosphino)ferrocenyl]ethyl methyl ether (**3a**) gave high yield of (*R*)-(−)-2,2′-dimethyl-1,1′-binaphthyl (**4a**) in up to 95% ee. Ferrocenylphosphine **3a** was also effective for the reaction of **1a** with 1-naphthyl bromide (**2b**) and that of (2-ethyl-1-naphthyl)magnesium bromide (**1c**) with **2b** to give corresponding cross-coupling products in 83 and 77% ee, respectively.

Optically active 1,1′-binaphthyl derivatives constitute an important class of compounds which have found extensive use in chiral auxiliaries for asymmetric synthesis,[2-6] and there has recently been an intense interest in obtaining the optically active binaphthyls by methods[7-10] other than those of optical resolution

(1) For part 5 in this series, see: Hayashi, T.; Kanehira, K.; Hagihara, T.; Kumada, M. *J. Org. Chem.* **1988**, *53*, 113.

(2) (a) For a pertinent review: Miyano, S.; Hashimoto, H. *Yuki Gosei Kagaku Kyokaishi* **1986**, *44*, 713. (b) For a recent review concerning asymmetric reactions: Nógrádi, M. *Stereoselective Synthesis*; VCH Verlag: Weinheim, 1987.

(3) For 2,2′-bisphosphine derivatives: (a) Takaya, H.; Mashima, K.; Koyano, K.; Yagi, M.; Kumobayashi, H.; Taketomi, T.; Akutagawa, S.; Noyori, R. *J. Org. Chem.* **1986**, *51*, 629. (b) Kitamura, M.; Ohkuma, T.; Inoue, S.; Sayo, N.; Kumobayashi, H.; Akutagawa, S.; Ohta, T.; Takaya, H.; Noyori, R. *J. Am. Chem. Soc.* **1988**, *110*, 629, and their previous papers cited therein.

(4) For 2,2′-diol and its derivatives: (a) Noyori, R.; Tomino, I.; Tanimoto, Y.; Nishizawa, M. *J. Am. Chem. Soc.* **1984**, *106*, 6709. Noyori, R.; Tomino, I.; Yamada, M.; Nishizawa, M. *J. Am. Chem. Soc.* **1984**, *106*, 6717. (b) Olivero, A. G.; Weidmann, B.; Seebach, D. *Helv. Chim. Acta* **1981**, *64*, 2485. Seebach, D.; Beck, A. K.; Roggo, S.; Wonnacott, A. *Chem. Ber.* **1985**, *118*, 3673. (c) Sakane, S.; Fujiwara, J.; Maruoka, K.; Yamamoto, H. *J. Am. Chem. Soc.* **1983**, *105*, 6154. (d) Maruoka, K.; Itoh, T.; Shirasaka, T.; Yamamoto, H. *J. Am. Chem. Soc.* **1988**, *110*, 310.

(5) For dihydrodinaphthoazepine derivatives: (a) Mazaleyrat, J. P.; Cram, D. J. *J. Am. Chem. Soc.* **1981**, *103*, 4585. (b) Maigrot, N.; Mazaleyrat, J. P.; Welvart, Z. *J. Org. Chem.* **1985**, *50*, 3916. (c) Hawkins, J. M.; Fu, G. C. *J. Org. Chem.* **1986**, *51*, 2820.

(6) For dicarboxylic acid esters and amides: Groves, J. T.; Myers, R. S. *J. Am. Chem. Soc.* **1983**, *105*, 5791.

0002-7863/88/1510-8153$01.50/0